Synthesis and Characterization of a Series of Iron Carbonyl Clusters Containing Selenium and Tellurium

Robert E. Bachman and Kenton H. Whitmire*

Department of Chemistry, Rice University, P.O. Box 1892, Houston, Texas 77251

Received November 24, 1993®

The reaction of TeO_2 with $Fe(CO)_5$/KOH/MeOH produces $[Te\{Fe(CO)_4\}_3]^{2-}$, which can be easily isolated as its $[PPN]^+$ salt, $[PPN]_2$[**I**]·0.5 THF, which crystallizes in the trigonal space group $P\bar{3}$ with $a = b = 25.447(4)$ Å, $c = 22.432(4)$ Å, $V = 12579.7(36)$ Å^3, and $Z = 6$. The Te atom is coordinated to three $Fe(CO)_4$ fragments in a pyramidal arrangement with an average Te–Fe distance of 2.642(8) Å and an average Fe–Te–Fe angle of 109.56(6)°. When $[PPN]_2$[**I**] is left in solution, it slowly converts to $[PPN]_2[TeFe_3(CO)_9]$ ($[PPN]_2$[**II**]). This process can accelerated by either mild photolysis or thermolysis. [**II**]$^{2-}$ can also be prepared from $[Et_4N]_2[Fe_2(CO)_8]$ and $TeCl_4$. $[Et_4N]_2$[**II**] crystallizes in the monoclinic space group $P2_1/n$ with $a = 24.79(2)$ Å, $b = 11.041(2)$ Å, $c = 25.209(11)$ Å, $b = 110.49(5)°$, $V = 6465.0(69)$ Å^3, and $Z = 8$. The tetrahedral cluster is composed of a "naked" Te atom capping a closed Fe_3 triangle. SeO_2 also reacts with $Fe(CO)_5$/KOH/MeOH, analogously to TeO_2, to produce a compound thought to be $[Se\{Fe(CO)_4\}_3]^{2-}$ ([**III**]$^{2-}$). [**III**]$^{2-}$ rapidly converts in solution to $[SeFe_3(CO)_9]^{2-}$ ([**IV**]$^{2-}$). $[PPN]_2$[**IV**]·CH_2Cl_2 crystallizes in the monoclinic space group Cc with $a = 29.393(6)$ Å, $b = 14.724(3)$ Å, $c = 21.477(4)$ Å, $b = 123.65(3)°$, $V = 7737.4(27)$, and $Z = 4$. [**IV**]$^{2-}$ was found to be isostructural with [**II**]$^{2-}$.

Introduction

Transition metal clusters which contain chalcogenide elements have been an active area of research for many years.[1] Much of this interest is generated by efforts to model both biological systems[2] and industrial catalysts used for hydrodesulfurization processes.[3] Much more is known about transition metal sulfide clusters than similar clusters which contain the heavier chalcogens.

The earliest systematic work with selenium- and tellurium-containing clusters was due to the efforts of Hieber and co-workers. They employed an acidic workup of reaction mixtures produced from TeO_2 and $Fe(CO)_5$/KOH/MeOH to prepare $Fe_3(CO)_9Te_2$;[4] however, they did not characterize the anionic species initially produced in this reaction. Rauchfuss and co-workers have examined the synthesis of chalcogen-containing clusters via similar methods. Notable results from their work include the first report of the reactive compound $Fe_2(CO)_6Te_2$[5] and the characterization of $(RC_5H_4)MoFe(CO)_5(Te_2Br)$,[6] which contains a hypervalent tellurium center. The Rauchfuss and Mathur research groups have prepared numerous heterometallic clusters, including $CpCoFe_2(CO)_6Te_2$,[7] $Fe_2(CO)_6Te_2Pt(PPh_3)_2$,[8] $Fe_2(CO)_6Te_2TiCp_2$,[9] and $Fe_2Ru_3(CO)_{17}Te_2$,[10] while studying the reactivity of $Fe_2(CO)_6Te_2$ and $Fe_3(CO)_9Te_2$.

More recently soluble polychalcogenide ions were employed for the synthesis of mixed-metal clusters. This strategy led to the preparation of a number of very interesting compounds, including $[Fe_5Te_4(CO)_{14}]^{2-}$,[11a] $[Fe_8Te_{10}(CO)_{20}]^{2-}$,[11a,b] $[Fe_4Se_4(CO)_{12}]^{2-}$,[11b] $[Fe_2(CO)_6Te_3]^{2-}$,[12] $[Cr_4Te_2(CO)_{20}]^{2-}$,[13] $[W_6Te_8(CO)_{18}]^{2-}$,[14] and $[Ru_6Te_{14}(CO)_{12}]^{2-}$.[15] In a complementary approach, we have noted the synthesis of $[Fe_2Te_4(CO)_6]^{2-}$ from $[Fe(CO)_4]^{2-}$ and elemental tellurium.[16]

We have been interested in the nature of the initial anionic species produced in reactions between reducing metal carbonylates and main group oxides and halides for quite some time. In the cases of In, Tl, Sn, Pb, As, Sb, and Bi, it has been shown that compounds having a central main group atom bonded to independent $Fe(CO)_4$ units are produced. This work is here extended to include the heavier chalcogens, where similar results are observed.

Experimental Section

General Procedures. All reactions and other manipulations were performed with oven-dried Schlenkware using standard techniques on a Schlenk line or in a Vacuum Atmospheres drybox under a dry nitrogen atmosphere unless otherwise noted. All solvents were dried and distilled under nitrogen prior to use: methanol (Mg); THF and ether (Na/Ph_2CO); hexanes ($LiAlH_4$); dichloromethane and acetonitrile (CaH_2). Bis(triphenylphosphine)nitrogen(1+) chloride, [PPN]Cl, was prepared according to literature methods.[17] $Fe(CO)_5$ (Aldrich), TeO_2 (Fisher), $TeCl_4$ (Strem), SeO_2 (K & K Laboratories), $[Et_4N]Br$ (Janssen), and KOH (EM Science) were used as received without further purification. Solution IR spectra were recorded in 0.1 mm path length CaF_2 cells on a Perkin-Elmer Model 1640 FT-IR spectrophotometer. ^1H and ^{13}C NMR spectra were obtained on a Bruker AF 300 spectrometer in CD_2Cl_2. FAB mass spectral analyses were performed on a VG Analytical Autospec 3000 using *m*-nitrobenzyl alcohol (mNBA) as a matrix. Elemental analyses were performed on a Carlo Erba Instruments NA 1500 Series 2 analyzer.

Synthesis of $[PPN]_2[Te\{Fe(CO)_4\}_3]$ ($[PPN]_2$[I**]).** All manipulations were performed under a carbon monoxide atmosphere and in the absence

* Author to whom correspondence should be addressed.

® Abstract published in *Advance ACS Abstracts,* May 1, 1994.

(1) For recent reviews see: (a) Roof, L. C.; Kolis, J. W. *Chem. Rev.* **1993,** *93,* 1037. (b) Ansari, M. A.; Ibers, J. A. *Coord. Chem. Rev.* **1990,** *100,* 223. (c) Compton, N. A.; Errington, R. J.; Norman, N. C. *Adv. Organomet. Chem.* **1990,** *31,* 91. (d) Whitmire, K. H. *J Coord. Chem. B.* **1988,** *17,* 95.
(2) (a) Coucouvanis, D. *Acc. Chem Res.* **1991,** *24,* 1. (b) Holm, R. H.; Ciurli, S.; Weigel, J. A. *Prog. Inorg. Chem.* **1990,** *38,* 1.
(3) Rakowski Dubois, M. *Chem. Rev.* **1989,** *89,* 1.
(4) Hieber, W.; Gruber, J. *Z. Anorg. Allg. Chem.* **1958,** *296,* 91.
(5) Lesch, D. A.; Rauchfuss, T. B. *Inorg. Chem.* **1981,** *20,* 3583.
(6) Bogan, L. E., Jr.; Rauchfuss, T. B.; Rheingold, A. L. *Inorg Chem.* **1985,** *24,* 3720.
(7) Bogan, L. E., Jr.; Lesch, D. A.; Rauchfuss, T. B. *J. Organomet Chem.* **1983,** *250,* 429.
(8) Lesch, D. A.; Rauchfuss, T. B. *J. Organomet. Chem.* **1980,** *199,* C6.
(9) Mathur, P.; Reddy, D. *J. Organomet. Chem.* **1990,** *385,* 363.
(10) Mathur, P.; Mavunkal, I. J.; Rheingold, A. L. *J. Chem. Soc., Chem. Commun.* **1989,** 382.
(11) (a) Roof, L. C.; Pennington, W. T.; Kolis, J. W. *Angew. Chem., Int. Ed. Engl.* **1992,** *31,* 913. (b) Haung, S.-P.; Kanatzidis, M. G. *Inorg. Chem.* **1993,** *32,* 821.
(12) Eichhorn, B. W.; Haushalter, R. C.; Merola, J. S. *Inorg Chem.* **1990,** *29,* 728.
(13) Roof, L. C.; Pennington, W. T.; Kolis, J. W. *Inorg Chem.* **1992,** *31,* 2056.
(14) Roof, L. C.; Pennington, W. T.; Kolis, J. W. *J. Am. Chem. Soc.* **1990,** *112,* 8172.
(15) Haung, S.-P.; Kanatzidis, M. G. *J. Am. Chem. Soc.* **1992,** *114,* 5477.
(16) Bachman, R. E.; Whitmire, K. H. *Organometallics* **1993,** *12,* 1988.
(17) Ruff, J. K.; Schlientz, W. D. *Inorg. Synth.* **1975,** *15,* 84.

0020-1669/94/1333-2527$04.50/0

Table 1. Crystal Data for $[PPN]_2[I]$, $[Et_4N]_2[II]$, and $[PPN]_2[IV]$

empirical, formula	$C_{86}H_{64}Fe_3N_2O_{125}P_4Te$	$C_{25}H_{40}Fe_3N_2O_9Te$	$C_{82}H_{62}Cl_2Fe_3N_2O_9P_4Se$
fw	1744.42	807.74	1660.63
T, K	223(2)	223(2)	293(2)
space group	$P\bar{3}$ (No. 147)	$P2_1/n$ (No. 14)	Cc (No. 9)
a, Å	25.447(4)	24.79(2)	29.393(6)
b, Å	25.447(4)	11.041(2)	14.724(3)
c, Å	22.432(4)	25.209(11)	21.477(4)
β, deg		110.49(5)	123.65(3)
V, Å^3	12 579.7(36)	6465.0(69)	7737.4(27)
Z	6	8	4
ρ_{calc}, g/cm^3	1.382	1.660	1.426
μ, mm^{-1}	0.989	2.263	1.235
$F(000)$	5304	3248	3384
data/param	8351/976	5981/716	5014/553
refinement	F^2	F	F^2
goodness-of-fit	1.067	2.174	1.022
residuals[a]	$R_1(F) = 0.0614$, $R_{2w}(F^2) = 0.1714$	$R(F) = 0.0534$, $R_w(F) = 0.0624$	$R_1(F) = 0.0571$, $R_{2w}(F^2) = 0.1324$

[a] The residuals are defined as follows: $R_{2w} = \{\sum[w(F_o^2 - F_c^2)^2]/\sum(wF_o^2)^2\}^{0.5}$, with $w = [\sum^2 F_o^2 + (a^*P)^2 + b^*P]^{-1}$ and $P = 0.33F_o^2 + 0.67F_c^2$; $R_1 = R = \sum||F_o| - |F_c||/\sum|F_o|$; $R_w = [\sum_w||F_o| - |F_c||^2/\sum|F_o|^2]^{0.5}$, with $w = [\sigma^2(F_o)]^{-1}$

of bright light. To a solution of 2.0 g (35.6 mmol) of KOH in 40 mL of methanol was added 1.0 mL (7.6 mmol) of $Fe(CO)_5$. After approximately 15 min, 0.40 g (2.5 mmol) of solid TeO_2 was added. The solution color immediately changed from pale yellow to deep red-brown. The reaction was allowed to continue for approximately 10 min, and then the product was precipitated by adding an excess (approximately 6 g) of [PPN]Cl. The precipitate was collected by filtration and dried in vacuo. The crude material was purified by dissolving it in minimal amounts of THF (20–30 mL) and precipitating it by adding three volumes of MeOH to yield 3.5 g (82% based on Te) of dark red-black microcrystalline powder. Single crystals suitable for structural determination were grown from a CO-saturated THF solution layered with methanol and held under 1–2 atm of CO in the dark for several days. IR (MeOH, cm^{-1}): 2024 w, 1992 s, 1920 sh, 1908 vs. IR (THF, cm^{-1}): 2020 w, 1985 vs, 1926 ms, 1900 s. ^{13}C NMR (CD_2Cl_2, ppm): 220.0 (CO), 134.1, 131.2 (J_{P-C} = 209 Hz), 128.0, 126.6. MS (negative-ion FABMS, mNBA): m/z 632, 548. Anal. Calcd for $C_{84}H_{60}Fe_3N_2O_{12}P_4Te$: C, 59.05; H, 3.54; N, 1.64. Found: C, 58.01; H, 4.09; N, 2.03.

Synthesis of $[PPN]_2[TeFe_3(CO)_9]$ ($[PPN]_2[II]$). Method 1. A solution of 2.0 g (1.17 mmol) of $[PPN]_2[I]$ in 35 mL of THF was placed in a photoreactor consisting of a water-jacketed 450-W Hanovia medium-pressure mercury vapor lamp and a cooling bath. The solution was irradiated for approximately 2 h. The product precipitated from solution as it was formed. It was collected by filtration and dried to give 1.56 g (82%) of dark red microcrystalline product.

Method 2. A solution prepared as in method 1 was refluxed (~70 °C) for 2–3 h. As above, the product precipitated from solution as it formed to yield 1.5 g (79%) of $[PPN]_2[II]$. The product was easily recrystallized by layering a concentrated solution in CH_2Cl_2 with two volumes of ether.

IR (CH_2Cl_2, cm^{-1}): 1992 w, 1924 vs, 1895 m, 1868 w, sh. ^{13}C NMR (CD_2Cl_2, ppm): 223.7 (CO), 134.0, 131.1 (J_{P-C} = 201 Hz), 128.0, 126.6. MS (negative-ion FABMS, mNBA): m/z 548, 492, 464. Anal. Calcd for $C_{81}H_{60}Fe_3N_2O_9P_4Te$: C, 59.89; H, 3.72; N, 1.72. Found: C, 60.39; H, 4.33; N, 2.12.

Synthesis of $[Et_4N]_2[TeFe_3(CO)_9]$, ($[Et_4N]_2[II]$). Acetonitrile solutions of $[Et_4N]_2[Fe_2(CO)_8]$ (2.98 g in 30 mL, 5.0 mmol) and $TeCl_4$ (0.67 g in 10 mL, 2.5 mmol) were prepared. The $TeCl_4$ solution was added to the iron carbonylate solution dropwise. The solution rapidly turned black, and a large amount of dark precipitate formed. After the addition was complete the reaction was allowed to continue for 2–3 h. The insoluble material was removed by filtration through Celite and the solvent removed under reduced pressure. The product was recovered by extracting the residues with CH_2Cl_2 (30 mL). The deep red CH_2Cl_2 solution was filtered to remove the solid particles and the volume reduced by about one-third. The product crystallized from solution at −20 °C over the course of several days, leaving unidentified impurities in solution. The isolated yield was 0.1 g (5.8% based on Te).

Synthesis of $[PPN]_2[Se\{Fe(CO)_4\}_3]$ ($[PPN]_2[III]$). A solution of $Fe(CO)_5$ and KOH in methanol was prepared as described above. Solid SeO_2 (0.28 g, 2.5 mmol) was added in one portion. The solution color immediately changed from pale yellow to deep red-brown. The initial infrared pattern was almost identical to that seen for $[I]^{2-}$, indicating the presence of $[III]^{2-}$ in solution. Crude samples of $[PPN]_2[III]$ can be isolated by rapidly precipitating material with excess [PPN]Cl. All attempts to purify this material further for complete spectral characterization resulted in rapid formation of $[PPN]_2[IV]$. IR (MeOH, cm^{-1}): 2040 w, 1996 m, 1932 s, 1897 vs.

Synthesis of $[PPN]_2[SeFe_3(CO)_9]$ ($[PPN]_2[IV]$). The procedure used to prepare $[III]^{2-}$ in solution was followed. After 5 min, the infrared spectrum indicated that a sizable amount of $[III]^{2-}$ had been transformed to $[IV]^{2-}$. After approximately 30 min, the transformation was complete. $[IV]^{2-}$ was isolated conveniently by precipitating it with excess [PPN]Cl and collecting the product by filtration. $[PPN]_2[IV]$ was purified by dissolving it in CH_2Cl_2, followed by precipitation with excess ether. The red microcrystalline product was collected by filtration and dried in vacuo. Crystals suitable for structural study were grown by slow diffusion of ether into a concentrated CH_2Cl_2 solution. Structural determination on well-dried crystals revealed the presence of lattice CH_2Cl_2. Yield (for $[PPN]_2[IV]\cdot CH_2Cl_2$, based on Se): 3.5g (84%). IR (CH_2Cl_2, cm^{-1}): 1995 w, 1926 vs, 1897 m, 1870 w, sh. ^{13}C NMR (CD_2Cl_2, ppm): 220.0 (CO), 134.2, 131.1 (J_{P-C} = 192 Hz), 127.9, 126.5. MS (negative-ion FABMS): m/z 499, 471, 444, 415. Anal. Calcd for $C_{86}H_{62}Cl_2Fe_3N_2O_{12}P_4Se$: C, 59.30; H, 3.76; N, 1.69. Found: C, 59.65; H, 4.15; N, 2.20.

Structural Determinations of $[PPN]_2[I]$, $[Et_4N]_2[II]$, and $[PPN]_2[IV]$. General Considerations. All crystals were mounted with epoxy cement on the tip of a glass fiber. Data were collected using the TEXSAN Automatic Data Collection Series[18] on a Rigaku AFC5S diffractometer using Mo Kα radiation (λ = 0.710 69Å). The crystallographic data collection parameters are summarized in Table 1. The data were corrected for Lorentz and polarization factors and for absorption using ψ scans. The analytical form of the scattering factors for the appropriate neutral atoms were corrected for both the real ($\Delta f'$) and imaginary ($\Delta f''$) components of anomalous dispersion.[19]

$[PPN]_2[I]\cdot 0.5THF$. A thin red-black hexagonal plate 0.2 × 0.1 × 0.3 mm^3 was chosen for data collection. The unit cell was determined from least-squares analysis of 25 reflections ($7° \le 2\theta \le 13°$). The space group $P\bar{3}$ (No. 147) was chosen on the basis of the Laue symmetry, the lack of systematic absences, and the intensity statistics. It was shown to be correct by satisfactory refinement of the data. The locations of the heavy atoms were determined using the Siemens SHELXTL PC software package.[20] The positions of all the other atoms were determined by successive least-squares refinements on F^2 using SHELXL-93.[21] All of the non-hydrogen atoms were refined anisotropically with the exception of the lattice solvent, which was refined isotropically, and the occupancy of the lattice solvent was refined. The hydrogen atoms were included in calculated positions by employing a riding model and a fixed isotropic thermal parameter. The final residuals of $R_1(F) = 0.0614$ and $R_{2w}(F^2) = 0.1714$ were based on 976 parameters and 6018 observed data ($I > 2\sigma(I)$), where R_1 is based on an equivalent refinement on F and R_{2w} is based on the actual refinement on F^2. Positional and equivalent isotropic

(18) *TEXSAN: Single Crystal Structure Analysis Software*, v. 5.0; Molecular Structure Corp.: Woodlands, TX, 1989.
(19) *International Tables for X-ray Crystallography*; Kynoch: Birmingham, England, 1974; Vol. 4, pp 99–101 and 149–150.
(20) *SHELXTL PC*, v 4.2; Siemens Crystallographic Research Systems: Madison, WI, 1990.
(21) Sheldrick, G. M. SHELXL-93. University of Goettingen, Germany, 1993.

Table 2. Selected Atomic Coordinates ($\times 10^4$) and Equivalent Isotropic Displacement Parameters ($Å^2 \times 10^3$) for $[PPN]_2[I]$

atom	x	y	z	U(eq)[a]
Te(1)	0	0	2927(1)	42(1)
Fe(1)	402(1)	−715(1)	2537(1)	44(1)
O(11)	−237(5)	−878(4)	1406(4)	85(3)
O(12)	1639(4)	315(4)	2686(5)	85(3)
O(13)	−260(5)	−1489(4)	3556(4)	92(3)
O(14)	794(4)	−1560(4)	2165(4)	80(3)
C(11)	13(5)	−802(5)	1854(6)	54(3)
C(12)	1149(6)	−91(6)	2621(6)	59(3)
C(13)	3(5)	−1171(5)	3157(6)	59(3)
C(14)	653(5)	−1216(5)	2325(5)	54(3)
Te(2)	3333	6667	2155(1)	32(1)
Fe(2)	2209(1)	6175(1)	1764(1)	38(1)
O(21)	2569(4)	5885(4)	625(4)	64(2)
O(22)	2271(3)	7359(4)	1842(4)	71(3)
O(23)	1901(4)	5366(4)	2794(4)	88(3)
O(24)	954(4)	5568(4)	1384(5)	96(3)
C(21)	2451(5)	6004(5)	1076(6)	46(3)
C(22)	2269(5)	6901(6)	1841(5)	50(3)
C(23)	2025(5)	5688(5)	2388(6)	56(3)
C(24)	1447(6)	5808(5)	1555(6)	57(3)
Te(3)	3333	6667	6715(1)	52(1)
Fe(3)	2232(1)	5879(1)	6324(1)	60(1)
O(31)	2737(4)	5767(5)	5208(5)	88(3)
O(32)	2166(6)	5171(6)	7363(6)	148(5)
O(33)	1881(4)	6813(5)	6370(6)	110(4)
O(34)	1023(5)	4994(5)	5921(6)	123(4)
C(31)	2569(6)	5825(6)	5653(7)	69(4)
C(32)	2208(7)	5472(7)	6945(7)	97(5)
C(33)	2038(5)	6462(6)	6368(6)	71(4)
C(34)	1510(7)	5339(6)	6086(7)	85(4)

[a] U(eq) is defined as one-third of the trace of the orthogonalized Uij tensor.

displacement parameters are given in Table 2, and selected bond distances, and angles are given in Table 5.

$[Et_4N]_2$[II]. A red-black needle $0.1 \times 0.1 \times 0.3$ mm^3 was chosen for study. The data were collected at 223 K. The unit cell was determined from 25 carefully centered reflections ($15° \leq 2\theta \leq 23°$). The space group, $P2_1/n$ (No. 14), was determined unambiguously from systematic absences. The heavy-atom positions were located by direct methods using SHELXS-86,[22] and the remaining atoms were located by successive least-squares refinements on F using the TEXSAN (5.0) structure solution package.[18] The non-hydrogen atoms were refined anisotropically, and the hydrogen atoms were included in calculated positions with their displacement parameters tied to the atom to which they were connected. The final residuals of $R = 0.0534$ and $R_w = 0.0624$ were based on 716 parameters and 5981 observed data ($I > 3\sigma(I)$) where both R and R_w are based on the refinement on F. Positional and equivalent isotropic displacement parameters are included in Table 3. Selected bond metricals are given in Table 6.

$[PPN]_2$[IV]·CH_2Cl_2. A red-brown chunk $0.3 \times 0.4 \times 0.3$ mm^3 was cut from a larger crystal and coated with epoxy cement . The unit cell was determined from least-squares analysis of 25 reflections ($6° \leq 2\theta \leq 12°$). The space group, Cc (No. 9), was indicated from the systematic absences and intensity statistics. This space group was chosen and shown to be correct by successful refinement of the structure. The heavy-atom positions were determined with the Siemens SHELXTL PC package.[20] The remaining atoms were located by successive least-squares refinements on F^2 using SHELXL-93.[21] The entire anion, along with the phosphorus and nitrogen atoms of the cation, was refined anisotropically. The remaining non-hydrogen atoms were refined isotropically, and the hydrogen atoms were included in calculated positions by employing a riding model with a fixed displacement parameter. During the final stages of refinement, the Flack parameter indicated that the crystal was probably composed of a racemic twin. Refinement using the twin routine of the SHELXL-93 package significantly improved the residuals. The final residuals of $R_1(F) = 0.0571$ and $R_{2w}(F^2) = 0.1324$ were based on 553 parameters and 3529 observed reflections ($I > 2\sigma(I)$). Positional and equivalent isotropic displacement parameters are given in Table 4. Selected bond metricals are included in Table 7.

(22) Sheldrick, G. M. In *Crystallographic Computing 3*; Sheldrick, G. M., Kruger, C., Goddard, R., Eds.; Oxford University Press: Oxford, England, 1985; pp 175–189.

Table 3. Selected Atomic Coordinates and Equivalent Isotropic Displacement Parameters for $[Et_4N]_2$[II]

atom	x	y	z	B(eq)[a]
Te(1)	0.48864(3)	0.25481(7)	0.11674(3)	2.93(3)
Fe(1)	0.57889(7)	0.1357(1)	0.13580(7)	2.68(7)
Fe(2)	0.55230(7)	0.2414(1)	0.21722(7)	2.92(7)
Fe(3)	0.57982(7)	0.3728(1)	0.14349(7)	3.19(7)
O(11)	0.5468(4)	−0.102(7)	0.1658(4)	4.3(4)
O(12)	0.7035(4)	0.115(1)	0.1869(5)	6.9(5)
O(13)	0.5716(4)	0.1012(8)	0.0188(4)	5.7(5)
O(21)	0.5047(4)	0.0354(7)	0.2577(4)	4.7(4)
O(22)	0.6693(4)	0.226(1)	0.2980(4)	6.7(5)
O(23)	0.5056(4)	0.4398(7)	0.2649(4)	4.7(4)
O(31)	0.5831(5)	0.4174(9)	0.0306(4)	7.3(6)
O(32)	0.7026(4)	0.395(1)	0.2094(6)	8.7(6)
O(33)	0.5490(3)	0.6044(7)	0.1808(4)	4.2(4)
C(11)	0.5587(5)	−0.007(1)	0.1523(5)	3.0(5)
C(12)	0.6555(6)	0.127(1)	0.1683(6)	4.5(6)
C(13)	0.5740(5)	0.116(1)	0.0643(6)	3.9(6)
C(21)	0.5230(5)	0.117(1)	0.2404(5)	3.2(5)
C(22)	0.6228(5)	0.234(1)	0.2646(5)	4.3(6)
C(23)	0.5242(5)	0.362(1)	0.2458(5)	3.3(5)
C(31)	0.5803(6)	0.400(1)	0.0755(7)	5.3(7)
C(32)	0.6540(6)	0.382(1)	0.1833(7)	5.8(7)
C(33)	0.5595(4)	0.512(1)	0.1649(5)	2.6(5)
Te(2)	0.09538(3)	0.06769(7)	0.05472(3)	2.92(3)
Fe(4)	0.13797(6)	0.2577(1)	0.03148(6)	2.62(6)
Fe(5)	0.20305(6)	0.0764(1)	0.08575(6)	2.56(6)
Fe(6)	0.14399(7)	0.2032(1)	0.13489(7)	2.67(6)
O(41)	0.0312(4)	0.3940(8)	−0.0027(4)	5.4(4)
O(42)	0.2112(3)	0.4713(7)	0.0592(4)	4.4(4)
O(43)	0.1453(4)	0.1841(8)	−0.0770(4)	5.0(4)
O(51)	0.2710(3)	−0.0329(7)	0.1937(3)	4.1(4)
O(52)	0.2067(3)	−0.1168(7)	0.0082(3)	4.3(4)
O(53)	0.2969(4)	0.2288(8)	0.0815(4)	4.6(4)
O(61)	0.2442(4)	0.3551(8)	0.1856(4)	5.3(4)
O(62)	0.1483(4)	0.0465(7)	0.2297(3)	4.0(4)
O(63)	0.0491(3)	0.3600(7)	0.1362(3)	3.7(4)
C(41)	0.0729(5)	0.340(1)	0.0095(5)	3.3(5)
C(42)	0.1822(5)	0.379(1)	0.0490(4)	3.4(5)
C(43)	0.1426(5)	0.214(1)	−0.0341(6)	3.6(5)
C(51)	0.2414(4)	0.010(1)	0.1507(5)	2.3(4)
C(52)	0.2045(4)	−0.037(1)	0.0374(5)	2.8(5)
C(53)	0.2559(5)	0.173(1)	0.0828(5)	3.8(5)
C(61)	0.2085(4)	0.3016(9)	0.1578(4)	1.5(2)
C(62)	0.1475(5)	0.107(1)	0.1926(5)	3.3(5)
C(63)	0.0880(5)	0.298(1)	0.1365(5)	2.9(5)

[a] $B(\text{eq}) = (8\pi^2/3) \sum_{i=1}^{3} \sum_{j=1}^{3} U_{ij} a_i^* a_j^* \vec{a}_i \vec{a}_j$.

Results

The reaction of TeO_2 with 3 equiv of $Fe(CO)_5$ in a KOH/methanol solution gives the anion $[Te\{Fe(CO)_4\}_3]^{2-}$ ($[I]^{2-}$), as the only carbonyl-containing product. Addition of [PPN]Cl causes precipitation of the cluster from solution in high yield. $[PPN]_2$[I] can be recrystallized from carbon monoxide saturated THF solutions layered with methanol and kept under 1–2 atm of additional CO. The recrystallization proceeds most effectively in the absence of light. The simple three-band infrared spectrum of $[I]^{2-}$ is consistent with the presence of isolated trigonal bipyramidal $Fe(CO)_4$ fragments. Negative-ion FAB mass spectral analysis gave an extremely weak signal for the parent ion and a much stronger signal for the parent ion minus 3 CO's. The rest of the mass spectral pattern showed the expected stepwise loss of CO down to the bare metal core. The ^{13}C NMR spectrum revealed only a single resonance in the carbonyl region at room temperature. The structure was confirmed by X-ray crystallography.

$[PPN]_2$[I] crystallizes in the trigonal space group $P\bar{3}$ (No. 147) with three independent anions lying on crystallographic 3-fold axes, two cations in general positions, and a molecule of lattice THF at approximately half-occupancy. A diagram showing the molecular geometry and labeling scheme for one independent anion is shown in Figure 1. The anion therefore has crystallographically imposed C_3 symmetry and is isostructural

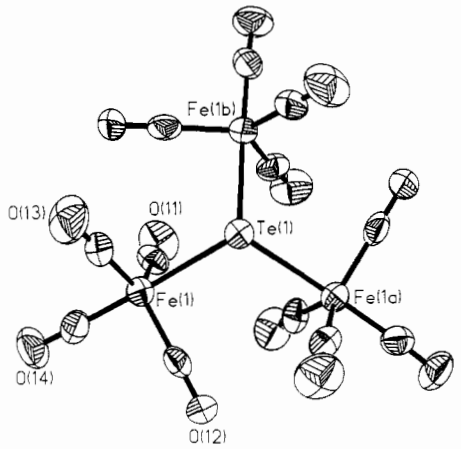

Figure 1. Diagram of one independent anion of $[PPN]_2[\mathbf{I}]$ showing the anisotropic displacement parameters (50% probability level) and atomic labeling scheme. Unlabeled atoms are related by symmetry to the labeled atoms, and the labeling for the carbons follows that used for the oxygens.

Table 4. Selected Atomic Coordinates ($\times 10^4$) and Equivalent Isotropic Displacement Parameters ($Å^2 \times 10^3$) for $[PPN]_2[\mathbf{II}]\cdot CH_2Cl_2$

atom	x	y	z	$U(eq)^a$
Se(1)	812(1)	4097(1)	7377(1)	60(1)
Fe(1)	1383(1)	2839(1)	7883(1)	49(1)
Fe(2)	1578(1)	4253(1)	7327(1)	45(1)
Fe(3)	1587(1)	4401(1)	8549(1)	53(1)
O(11)	981(7)	1928(11)	8669(7)	120(6)
O(12)	2491(5)	2097(8)	8720(8)	92(4)
O(13)	972(5)	1676(8)	6574(6)	76(3)
O(21)	2766(5)	3879(7)	8149(6)	68(3)
O(22)	1586(6)	6157(8)	6937(8)	102(5)
O(23)	1225(5)	3545(8)	5858(7)	73(3)
O(31)	2732(4)	3977(8)	9675(6)	78(3)
O(32)	1735(8)	6364(9)	8635(8)	122(6)
O(33)	1115(7)	4195(13)	9425(9)	135(6)
C(11)	1144(7)	2299(13)	8357(10)	75(5)
C(12)	2061(7)	2409(10)	8392(10)	66(5)
C(13)	1122(6)	2132(11)	7081(9)	57(4)
C(21)	2296(6)	4026(9)	7828(8)	46(4)
C(22)	1586(6)	5409(12)	7110(8)	58(4)
C(23)	1366(6)	3822(10)	6458(9)	52(4)
C(31)	2273(7)	4114(11)	9212(8)	58(4)
C(32)	1666(8)	5557(13)	8589(9)	73(5)
C(33)	1318(7)	4269(14)	9087(10)	82(5)

^{a} $U(eq)$ is defined as one-third of the trace of the orthogonalized U_{ij} tensor.

and isomorphous with the isoelectronic complex $[PPN]_2[HAs\{Fe(CO)_4\}_3]\cdot 0.5THF$ reported elsewhere.[23] The Te–Fe bonds average 2.642(8) Å while the Fe–Te–Fe angles average 109.56(6) Å. The Fe–C and C–O distances are all normal ranging from 1.72(2) to 1.79(1) Å and from 1.13(1) to 1.18(2) Å, respectively.

When solutions of $[\mathbf{I}]^{2-}$ in THF are left to stand at room temperature, the anion quantitatively loses three molecules of CO with the concomitant formation of three iron–iron bonds to yield $[PPN]_2[TeFe_3(CO)_9]$ ($[PPN]_2[\mathbf{II}]$), which precipitates from solution. This reaction can be accelerated considerably either by photolysis with a mercury vapor lamp or by warming the solution. The $[Et_4N]^+$ salt of this *closo*-tetrahedral anion is also formed by the reaction of $[Et_4N]_2[Fe_2(CO)_8]$ with 1 equiv of $TeCl_4$ in CH_3CN. The synthesis of $[\mathbf{II}]^{2-}$ from K_2Te and $Fe(CO)_5$ has also been reported.[1a] It is interesting that $[\mathbf{I}]^{2-}$ is sufficiently labile in solution that, even when the precautions listed above are taken, small amounts of $[\mathbf{II}]^{2-}$ will invariably form. $[PPN]_2[\mathbf{II}]$ can be conveniently recrystallized from CH_2Cl_2 solutions layered with ether while $[Et_4N]_2[\mathbf{II}]$ is recrystallized from concentrated solutions of CH_2Cl_2 held at −20 °C. Negative-ion FABMS gives a clean signal for the parent ion with the appropriate isotopic distribution pattern. As with $[PPN]_2[\mathbf{I}]$, sequential loss of CO to the bare metal core is also observed,. The ^{13}C NMR exhibited only one signal in the carbonyl region at 223 ppm. An X-ray crystallographic study was performed on $[Et_4N]_2[\mathbf{II}]$ to confirm the structure.

(23) Bachman, R. E.; Miller, S. K.; Whitmire, K. H. *Inorg. Chem.*, Submitted for publication.

Table 5. Selected Bond Distances (Å) and Angles (deg) for $[PPN]_2[\mathbf{I}]^a$

A. Distances

Te(1)–Fe(1)	2.642(2)	O(21)–C(21)	1.138(12)
Fe(1)–C(14)	1.753(13)	O(22)–C(22)	1.162(13)
Fe(1)–C(13)	1.770(14)	O(23)–C(23)	1.160(13)
Fe(1)–C(11)	1.776(14)	O(24)–C(24)	1.152(13)
Fe(1)–C(12)	1.774(14)	Te(3)–Fe(3)	2.651(2)
O(11)–C(11)	1.152(13)	Fe(3)–C(32)	1.72(2)
O(12)–C(12)	1.166(13)	Fe(3)–C(34)	1.74(2)
O(13)–C(13)	1.167(13)	Fe(3)–C(31)	1.77(2)
O(14)–C(14)	1.159(13)	Fe(3)–C(33)	1.78(2)
Te(2)–Fe(2)	2.6344(14)	O(31)–C(31)	1.125(14)
Fe(2)–C(24)	1.744(13)	O(32)–C(32)	1.18(2)
Fe(2)–C(23)	1.769(13)	O(33)–C(33)	1.146(14)
Fe(2)–C(22)	1.787(13)	O(34)–C(34)	1.16(2)
Fe(2)–C(21)	1.793(13)		

B. Angles

Fe(1)–Te(1)–Fe(1)*	109.58(4)	C(23)–Fe(2)–Te(2)	85.0(4)
C(14)–Fe(1)–C(13)	91.9(5)	C(22)–Fe(2)–Te(2)	88.1(3)
C(14)–Fe(1)–C(11)	93.3(5)	C(21)–Fe(2)–Te(2)	88.8(3)
C(13)–Fe(1)–C(11)	119.6(5)	O(21)–C(21)–Fe(2)	175.7(10)
C(14)–Fe(1)–C(12)	93.6(5)	O(22)–C(22)–Fe(2)	173.3(10)
C(13)–Fe(1)–C(12)	120.6(6)	O(23)–C(23)–Fe(2)	179.5(13)
C(11)–Fe(1)–C(12)	119.0(6)	O(24)–C(24)–Fe(2)	176.1(12)
C(14)–Fe(1)–Te(1)	176.1(4)	Fe(3)–Te(3)–Fe(3)*	109.60(5)
C(13)–Fe(1)–Te(1)	84.2(4)	C(32)–Fe(3)–C(34)	93.8(7)
C(12)–Fe(1)–Te(1)	87.7(3)	C(32)–Fe(3)–C(31)	120.9(7)
C(11)–Fe(1)–Te(1)	89.3(4)	C(34)–Fe(3)–C(31)	92.2(7)
O(11)–C(11)–Fe(1)	177.3(11)	C(32)–Fe(3)–C(33)	121.0(7)
O(12)–C(12)–Fe(1)	178.9(12)	C(34)–Fe(3)–C(33)	93.1(6)
O(13)–C(13)–Fe(1)	177.7(11)	C(31)–Fe(3)–C(33)	117.3(6)
O(14)–C(14)–Fe(1)	176.6(11)	C(32)–Fe(3)–Te(3)	83.8(5)
Fe(2)–Te(2)–Fe(2)*	109.49(4)	C(34)–Fe(3)–Te(3)	177.5(5)
C(24)–Fe(2)–C(23)	90.2(5)	C(31)–Fe(3)–Te(3)	88.3(5)
C(24)–Fe(2)–C(22)	94.3(5)	C(33)–Fe(3)–Te(3)	88.9(4)
C(23)–Fe(2)–C(22)	120.2(5)	O(31)–C(31)–Fe(3)	174.4(13)
C(24)–Fe(2)–C(21)	93.7(5)	O(32)–C(32)–Fe(3)	177(2)
C(23)–Fe(2)–C(21)	120.9(5)	O(33)–C(33)–Fe(3)	175.3(13)
C(22)–Fe(2)–C(21)	118.2(5)	O(34)–C(34)–Fe(3)	177.5(13)
C(24)–Fe(2)–Te(2)	175.3(4)		

^{a} An asterisk denotes a symmetry-related atom.

The crystallographic study of $[Et_4N]_2[\mathbf{II}]$ crystallizes in the monoclinic space group $P2_1/n$ (No. 14) with two anions and four cations occupying the asymmetric unit. The two independent anions are structurally identical within the experimental error, and no intermolecular contacts exist between them. Figure 2 shows the molecular geometry and labeling scheme for one of the anions. The Te–Fe and the Fe–Fe distances average 2.49(2) and 2.631(5) Å, respectively. The Fe–Te–Fe angles average 63.8(3),° and the Te–Fe–Fe angles average 58.1(5)°. The Fe–Fe–Fe angles are very close to 60°, ranging from 59.79(7) to 60.26(7)°.

The reaction of SeO_2 with methanol solutions of $Fe(CO)_5$ and KOH proceeds similarly to that seen with TeO_2. The initial IR spectrum gives a ν_{CO} pattern which is almost superimposible over that of $[\mathbf{I}]^{2-}$. It is believed that the species in solution is $[Se\{Fe(CO)_4\}_3]^{2-}$ ($[\mathbf{III}]^{2-}$). This material can be isolated in crude form by immediate precipitation with [PPN]Cl. In less than 10 min the solution spectrum shows the formation of $[\mathbf{IV}]^{2-}$. If the solution is left to stand for approximately 1 h, the conversion is complete. The closed cluster $[\mathbf{IV}]^{2-}$ is easily isolated by precipitation with [PPN]Cl. If $[PPN]_2[\mathbf{III}]$ is dissolved in THF, $[PPN]_2[\mathbf{IV}]$ rapidly precipitates even if the solvent is presaturated with CO and all manipulations are performed under an atmosphere of CO. Thus far all attempts to crystallize salts of $[\mathbf{III}]^{2-}$ for

Table 6. Selected Bond Distances (Å) and Angles (deg) for $[Et_4N]_2$[II]

A. Distances

Te(1)–Fe(1)	2.493(3)	Te(2)–Fe(4)	2.509(2)	Fe(3)–C(31)	1.75(2)	Fe(6)–C(61)	1.85(1)
Te(1)–Fe(2)	2.476(2)	Te(2)–Fe(5)	2.507(3)	Fe(3)–C(32)	1.76(1)	Fe(6)–C(62)	1.78(1)
Te(1)–Fe(3)	2.489(3)	Te(2)–Fe(6)	2.464(2)	Fe(3)–C(33)	1.76(1)	Fe(6)–C(63)	1.75(1)
Fe(1)–Fe(2)	2.638(3)	Fe(4)–Fe(5)	2.633(2)	O(11)–C(11)	1.17(2)	O(41)–C(41)	1.14(1)
Fe(1)–Fe(3)	2.625(2)	Fe(4)–Fe(6)	2.628(3)	O(12)–C(12)	1.13(2)	O(42)–C(42)	1.22(2)
Fe(1)–C(11)	1.75(1)	Fe(4)–C(41)	1.76(1)	O(13)–C(13)	1.14(2)	O(43)–C(43)	1.15(2)
Fe(1)–C(12)	1.79(1)	Fe(4)–C(42)	1.69(1)	O(21)–C(21)	1.16(2)	O(51)–C(51)	1.18(1)
Fe(1)–C(13)	1.78(1)	Fe(4)–C(43)	1.76(1)	O(22)–C(22)	1.17(1)	O(52)–C(52)	1.16(1)
Fe(2)–Fe(3)	2.630(3)	Fe(5)–Fe(6)	2.629(3)	O(23)–C(23)	1.15(2)	O(53)–C(53)	1.20(2)
Fe(2)–C(21)	1.75(1)	Fe(5)–C(51)	1.74(1)	O(31)–C(31)	1.17(2)	O(61)–C(61)	1.09(1)
Fe(2)–C(22)	1.74(1)	Fe(5)–C(52)	1.76(1)	O(32)–C(32)	1.16(2)	O(62)–C(62)	1.14(2)
Fe(2)–C(23)	1.77(1)	Fe(5)–C(53)	1.71(1)	O(33)–C(33)	1.16(1)	O(63)–C(63)	1.18(1)

B. Angles

Fe(1)–Te(1)–Fe(2)	64.12(8)	Fe(4)–Te(2)–Fe(5)	63.33(6)	Fe(3)–Fe(2)–C(23)	96.2(4)	Fe(6)–Fe(5)–C(53)	104.5(5)
Fe(1)–Te(1)–Fe(3)	63.59(7)	Fe(4)–Te(2)–Fe(6)	63.81(6)	C(21)–Fe(2)–C(22)	99.7(6)	C(51)–Fe(5)–C(52)	102.3(5)
Fe(2)–Te(1)–Fe(3)	63.96(8)	Fe(5)–Te(2)–Fe(6)	63.83(7)	C(21)–Fe(2)–C(23)	100.8(6)	C(51)–Fe(5)–C(53)	97.4(5)
Te(1)–Fe(1)–Fe(2)	57.62(7)	Te(2)–Fe(4)–Fe(5)	58.31(7)	C(22)–Fe(2)–C(23)	101.6(6)	C(52)–Fe(5)–C(53)	102.3(6)
Te(1)–Fe(1)–Fe(3)	58.13(6)	Te(2)–Fe(4)–Fe(6)	57.27(6)	Te(1)–Fe(3)–Fe(1)	58.28(6)	Te(2)–Fe(6)–Fe(4)	58.92(6)
Te(1)–Fe(1)–C(11)	102.1(4)	Te(2)–Fe(4)–C(41)	95.1(4)	Te(1)–Fe(3)–Fe(2)	57.77(7)	Te(2)–Fe(6)–Fe(5)	58.89(7)
Te(1)–Fe(1)–C(12)	148.6(4)	Te(2)–Fe(4)–C(42)	152.9(4)	Te(1)–Fe(3)–C(31)	98.3(5)	Te(2)–Fe(6)–C(61)	137.1(4)
Te(1)–Fe(1)–C(13)	97.6(4)	Te(2)–Fe(4)–C(43)	99.2(4)	Te(1)–Fe(3)–C(32)	148.5(5)	Te(2)–Fe(6)–C(62)	100.2(4)
Fe(2)–Fe(1)–Fe(3)	59.96(7)	Fe(5)–Fe(4)–Fe(6)	59.95(7)	Te(1)–Fe(3)–C(33)	102.1(4)	Te(2)–Fe(6)–C(63)	102.6(3)
Fe(2)–Fe(1)–C(11)	92.5(4)	Fe(5)–Fe(4)–C(41)	151.7(4)	Fe(1)–Fe(3)–Fe(2)	60.26(7)	Fe(4)–Fe(6)–Fe(5)	60.12(7)
Fe(2)–Fe(1)–C(12)	100.5(5)	Fe(5)–Fe(4)–C(42)	104.1(4)	Fe(1)–Fe(3)–C(31)	96.0(4)	Fe(4)–Fe(6)–C(61)	85.3(3)
Fe(2)–Fe(1)–C(13)	153.8(4)	Fe(5)–Fe(4)–C(43)	92.8(4)	Fe(1)–Fe(3)–C(32)	94.7(4)	Fe(4)–Fe(6)–C(62)	156.5(4)
Fe(3)–Fe(1)–C(11)	151.4(4)	Fe(6)–Fe(4)–C(41)	99.0(4)	Fe(1)–F(3)–C(33)	153.8(4)	Fe(4)–Fe(6)–C(63)	96.7(4)
Fe(3)–Fe(1)–C(12)	92.2(4)	Fe(6)–Fe(4)–C(42)	96.7(4)	Fe(2)–Fe(3)–C(31)	152.1(4)	Fe(5)–Fe(6)–C(63)	155.1(4)
Fe(3)–Fe(1)–C(13)	101.2(4)	Fe(6)–Fe(4)–C(43)	150.1(4)	Fe(2)–Fe(3)–C(32)	96.1(6)	C(61)–Fe(6)–C(62)	107.9(5)
C(11)–Fe(1)–C(12)	100.9(6)	C(41)–Fe(4)–C(42)	96.6(6)	Fe(2)–Fe(3)–C(33)	95.2(4)	C(61)–Fe(6)–C(63)	104.3(5)
C(11)–Fe(1)–C(13)	101.9(5)	C(41)–Fe(4)–C(43)	101.5(5)	C(31)–Fe(3)–C(32)	100.6(8)	Fe(5)–Fe(6)–C(61)	84.0(4)
C(12)–Fe(1)–C(13)	98.2(7)	C(42)–Fe(4)–C(43)	102.3(6)	C(31)–Fe(3)–C(33)	104.5(6)	Fe(5)–Fe(6)–C(62)	101.0(4)
Te(1)–Fe(2)–Fe(1)	58.26(7)	Te(2)–Fe(5)–Fe(4)	58.35(6)	C(32)–Fe(3)–C(33)	97.3(6)	C(62)–Fe(6)–C(63)	98.7(6)
Te(1)–Fe(2)–Fe(3)	58.27(7)	Te(2)–Fe(5)–Fe(6)	57.28(6)	Fe(1)–C(11)–O(11)	177.0(9)	Fe(4)–C(41)–O(41)	178(1)
Te(1)–Fe(2)–C(21)	101.4(3)	Te(2)–Fe(5)–C(51)	116.6(4)	Fe(1)–C(12)–O(12)	175(1)	Fe(4)–C(42)–O(42)	175.6(9)
Te(1)–Fe(2)–C(22)	146.4(5)	Te(2)–Fe(5)–C(52)	92.0(4)	Fe(1)–C(13)–O(13)	179(1)	Fe(4)–C(43)–O(43)	179(1)
Te(1)–Fe(2)–C(23)	99.8(3)	Te(2)–Fe(5)–C(53)	139.3(4)	Fe(2)–C(21)–O(21)	177.6(9)	Fe(5)–C(51)–O(51)	175(1)
Fe(1)–Fe(2)–Fe(3)	59.79(7)	Fe(4)–Fe(5)–Fe(6)	59.93(7)	Fe(2)–C(22)–O(22)	177(1)	Fe(5)–C(52)–O(52)	176(1)
Fe(1)–Fe(2)–C(21)	99.2(4)	Fe(4)–Fe(5)–C(51)	147.4(4)	Fe(2)–C(23)–O(23)	179(1)	Fe(5)–C(53)–O(53)	172(1)
Fe(1)–Fe(2)–C(22)	92.8(5)	Fe(4)–Fe(5)–C(52)	109.9(3)	Fe(3)–C(31)–O(31)	177(1)	Fe(6)–C(61)–O(61)	159(1)
Fe(1)–Fe(2)–C(23)	153.0(4)	Fe(4)–Fe(5)–C(53)	81.0(4)	Fe(3)–C(32)–O(32)	176(1)	Fe(6)–C(62)–O(62)	178(1)
Fe(3)–Fe(2)–C(21)	155.7(4)	Fe(6)–Fe(5)–C(51)	89.5(4)	Fe(3)–C(33)–O(33)	176.6(8)	Fe(6)–C(63)–O(63)	177.8(9)
Fe(3)–Fe(2)–C(22)	93.7(5)	Fe(6)–Fe(5)–C(52)	148.9(4)				

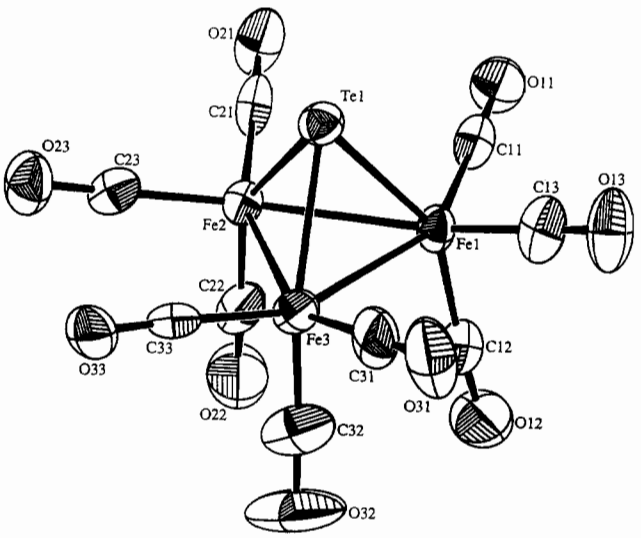

Figure 2. Diagram of one independent anion of $[Et_4N]_2$[II] showing the anisotropic displacement parameters (50% probability level) and atomic labeling scheme.

crystallographic analysis have resulted in the formation of salts of $[IV]^{2-}$. Negative ion FABMS analysis of crude samples of $[PPN]_2$[III] do not reveal a parent ion but show the parent less three CO fragments along with sequential loss of CO from this signal down to a bare metal core. This spectrum is identical with that seen for salts of $[IV]^{2-}$.

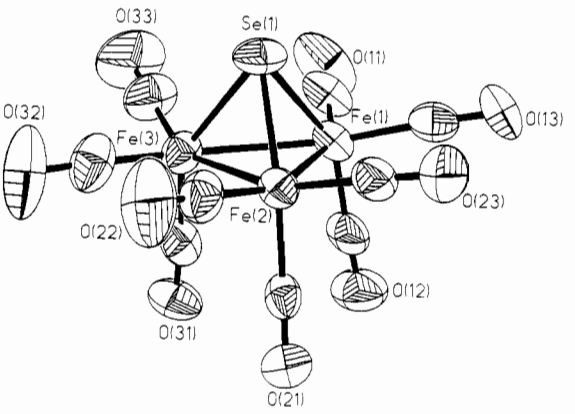

Figure 3. Diagram of the anion of $[PPN]_2$[IV] showing the anisotropic displacement parameters (50% probability level) and atomic labeling scheme. The labeling for the carbons follows that used for the oxygens.

$[PPN]_2$[IV] can be conveniently crystallized from a dichloromethane solution layered with ether. It crystallizes in the accentric space group *Cc* (No. 9) as a racemic twin. The asymmetric unit is composed of one anion, two cations, and a lattice CH_2Cl_2 molecule. The molecular geometry and atomic labeling scheme for the cluster are shown in Figure 3. The Se–Fe distances average 2.322(4) Å, and the Fe–Fe distances average 2.610(11) Å. The Fe–Se–Fe angles average 68.4(3)°, and the Se–Fe–Fe angles average 55.8(2)°. The Fe–Fe–Fe angles are again almost exactly 60°, ranging from 59.51(8) to 60.27(8)°. The Fe–C and C–O distances are also normal.

Table 7. Selected Bond Distances (Å) and Angles (deg) for $[PPN]_2[IV]\cdot CH_2Cl_2$

A. Distances

Se(1)–Fe(3)	2.318(3)	Fe(3)–C(32)	1.71(2)
Se(1)–Fe(2)	2.323(3)	Fe(3)–C(33)	1.74(2)
Se(1)–Fe(1)	2.326(3)	Fe(3)–C(31)	1.76(2)
Fe(1)–C(11)	1.72(2)	O(11)–C(11)	1.16(2)
Fe(1)–C(12)	1.78(2)	O(12)–C(12)	1.15(2)
Fe(1)–C(13)	1.78(2)	O(13)–C(13)	1.14(2)
Fe(1)–Fe(3)	2.597(3)	O(21)–C(21)	1.17(2)
Fe(1)–Fe(2)	2.616(3)	O(22)–C(22)	1.16(2)
Fe(2)–C(23)	1.73(2)	O(23)–C(23)	1.19(2)
Fe(2)–C(22)	1.77(2)	O(31)–C(31)	1.17(2)
Fe(2)–C(21)	1.79(2)	O(32)–C(32)	1.20(2)
Fe(2)–Fe(3)	2.617(3)	O(33)–C(33)	1.17(2)

B. Angles

Fe(3)–Se(1)–Fe(2)	68.65(8)	C(22)–Fe(2)–Fe(3)	100.9(5)
Fe(3)–Se(1)–Fe(1)	68.01(8)	C(21)–Fe(2)–Fe(3)	93.4(5)
Fe(2)–Se(1)–Fe(1)	68.48(8)	Se(1)–Fe(2)–Fe(3)	55.58(8)
C(11)–Fe(1)–C(12)	99.1(8)	Fe(1)–Fe(2)–Fe(3)	59.51(8)
C(11)–Fe(1)–C(13)	101.7(7)	C(32)–Fe(3)–C(33)	100.1(9)
C(12)–Fe(1)–C(13)	97.1(7)	C(32)–Fe(3)–C(31)	97.8(8)
C(11)–Fe(1)–Se(1)	102.6(6)	C(33)–Fe(3)–C(31)	100.0(8)
C(12)–Fe(1)–Se(1)	147.7(5)	C(32)–Fe(3)–Se(1)	105.7(6)
C(13)–Fe(1)–Se(1)	101.5(5)	C(33)–Fe(3)–Se(1)	99.5(6)
C(11)–Fe(1)–Fe(3)	97.4(6)	C(31)–Fe(3)–Se(1)	146.1(5)
C(12)–Fe(1)–Fe(3)	98.0(5)	C(32)–Fe(3)–Fe(1)	153.0(6)
C(13)–Fe(1)–Fe(3)	153.4(5)	C(33)–Fe(3)–Fe(1)	102.5(7)
Se(1)–Fe(1)–Fe(3)	55.85(8)	C(31)–Fe(3)–Fe(1)	92.6(5)
C(11)–Fe(1)–Fe(2)	154.5(7)	Se(1)–Fe(3)–Fe(1)	56.14(7)
C(12)–Fe(1)–Fe(2)	96.3(5)	C(32)–Fe(3)–Fe(2)	93.4(6)
C(13)–Fe(1)–Fe(2)	96.3(5)	C(33)–Fe(3)–Fe(2)	154.5(6)
Se(1)–Fe(1)–Fe(2)	55.71(7)	C(31)–Fe(3)–Fe(2)	99.4(5)
Fe(3)–Fe(1)–Fe(2)	60.27(8)	Se(1)–Fe(3)–Fe(2)	55.77(7)
C(23)–Fe(2)–C(22)	96.8(7)	Fe(1)–Fe(3)–Fe(2)	60.22(8)
C(23)–Fe(2)–C(21)	100.4(7)	O(11)–C(11)–Fe(1)	179(2)
C(22)–Fe(2)–C(21)	98.9(7)	O(12)–C(12)–Fe(1)	177.2(14)
C(23)–Fe(2)–Se(1)	103.5(5)	O(13)–C(13)–Fe(1)	177.6(14)
C(22)–Fe(2)–Se(1)	105.2(5)	O(21)–C(21)–Fe(2)	179.3(13)
C(21)–Fe(2)–Se(1)	143.5(5)	O(22)–C(22)–Fe(2)	177.1(14)
C(23)–Fe(2)–Fe(1)	99.3(5)	O(23)–C(23)–Fe(2)	178.3(13)
C(22)–Fe(2)–Fe(1)	157.6(5)	O(31)–C(31)–Fe(3)	175.7(14)
C(21)–Fe(2)–Fe(1)	93.5(5)	O(32)–C(32)–Fe(3)	178(2)
Se(1)–Fe(2)–Fe(1)	55.81(8)	O(33)–C(33)–Fe(3)	177(2)
C(23)–Fe(2)–Fe(3)	155.5(5)		

Discussion

Structures of $[PPN]_2[I]$, $[Et_4N]_2[II]$, and $[PPN]_2[IV]$. The Te–Fe bond distances in $[PPN]_2[I]$ (2.642(8) Å (average)) are slightly longer than those observed for other known clusters: $Fe_3(CO)_9Te_2$ (2.532(9) Å),[24] $Fe_3(CO)_{10}Te_2$ (2.566(6) Å),[25] $Fe_2(CO)_6Te_2CH_2$ (2.546(4) Å),[26] $Fe_2(CO)_6Te_2$ (2.543(2) Å),[27] and $[K(crypt)]_2[Fe_2(CO)_6Te_3]$ (2.572(14) Å).[12] There are a few compounds with comparable Fe–Te distances, including $[PPN][Fe(CO)_3(TePh)_3]$, with an average distance of 2.630(5) Å,[28] and $[Ph_4P]_2[Fe_8Te_{10}(CO)_{20}]$, which contains bonds ranging from 2.587(2) to 2.652(2) Å.[11] The most striking comparison, however, is between $[I]^{2-}$ and $[II]^{2-}$. The Te–Fe distances in $[II]^{2-}$ average 2.49 Å, or approximately 0.15 Å shorter than that seen in $[I]^{2-}$. The significantly longer Te–Fe bond in $[I]^{2-}$ is most likely caused by steric crowding of the bulky $Fe(CO)_4$ groups. This effect is seen in other open framework metal carbonyl clusters (see Table 8) such as $[Et_4N]_3[SbFe_4(CO)_{16}]$,[29] $[Et_4N]_3[BiFe_4(CO)_{16}]$,[30] and $BiCo_3(CO)_{12}$.[31] In all three of these cases, the main group metal bonds are between 0.1 and 0.2 Å longer in the open framework clusters than in closely related *closo* clusters which have also been structurally characterized: $[Et_4N]_2[HSbFe_4(CO)_{13}]$,[29] $[Et_4N][H_2SbFe_4(CO)_{13}]$,[29] $[Et_4N][BiFe_3(CO)_9(\mu\text{-}CO)]$,[32] and $BiCo_3(CO)_9$,[33] respectively.

Table 8. Selected Average Bond Distances (Å) for Representative Main Group Metal Clusters

complex	E–M	M–M	ref
$[Te\{Fe(CO)_4\}_3]^{2-}$	2.642(8)		*a*
$[TeFe_3(CO)_9]^{2-}$	2.490(2)	2.631(5)	*a*
$[SeFe_3(CO)_9]^{2-}$	2.322(9)	2.610(11)	*a*
$[HAs\{Fe(CO)_4\}_3]^{2-}$	2.460(7)		23
$As_2Fe_3(CO)_9$	2.348(2)	2.623(4)	39
$[Sb\{Fe(CO)_4\}_4]^{3-}$	2.666(3)		29
$[HSbFe_4(CO)_{13}]^{2-}$	2.467(7)[b]	2.733(26)	29
	2.521(2)[c]		
$[H_2SbFe_4(CO)_{13}]^{-}$	2.479(26)[b]	2.764(26)	29
	2.507(8)[c]		
$[SbFe_4(CO)_{14}]^{-}$	2.498(30)[b]	2.675(13)	40
	2.481(3)[c]		
$[Bi\{Fe(CO)_4\}_4]^{3-}$	2.750		30
$[BiFe_3(CO)_{10}]^{-}$	2.650(2)	2.642(7)	32
$Bi\{Co(CO)_4\}_3$	2.766		31
$BiCo_3(CO)_9$	2.613(6)	2.52(1)	33

[a] This work. [b] E–M bonds within the cluster core. [c] Bond to an external metal fragment.

The Se–Fe distances in $[PPN]_2[IV]$ average 2.322(4) Å. This is approximately equivalent to the average distances seen in $Fe_3(CO)_9Se_2$ (2.35(1) Å)[34] and $Fe_2(CO)_6Se_2$ (2.364 (11) Å)[35] and slightly shorter than that seen for $Fe_2(CO)_6Se_2HC_2Ph$ (2.384 (5) Å).[36] The inherent instability of $[PPN]_2[III]$ relative to its transformation to $[PPN]_2[IV]$ is explained by considering these bond metricals along with those observed for $[PPN]_2[I]$. The shorter Se–Fe distances in $[III]^{2-}$ versus the Te–Fe distances in $[I]^{2-}$ should result in a higher degree of steric crowding. This increased steric crowding would enhance the driving force for CO dissociation and therefore the conversion of $[III]^{2-}$ into $[IV]^{2-}$.

An interesting comparison can be made among $[PPN]_2[I]$, $[PPN]_2[III]$, and the isostructural and isoelectronic cluster $[PPN]_2[HAs\{Fe(CO)_4\}_3]$, which is produced in the reaction of $NAsO_2$ with $Fe(CO)_5$/KOH in methanol.[23] In contrast to $[PPN]_2[I]$, which slowly coverts to $[PPN]_2[II]$, and $[PPN]_2[III]$, which exists only briefly in solution, $[PPN]_2[HAs\{Fe(CO)_4\}_3]$ is completely inert to CO loss at room temperature. This is true even though the As–Fe bond is only 2.46 Å. The comparatively large stablity of this arsenic analog is probably the result of a combination of electronic and steric considerations. It is generally accepted that the steric demand of a lone pair is greater than that of a hydride ligand. This effect can be seen structurally in the Fe–E–Fe angle, which is 115.6° for the arsenic cluster versus 109.6° for $[PPN]_2[I]$. It appears that the effect of the lone pair is to force the Te–Fe bonds toward the closed structure. The wider Fe–E–Fe angles also help to relieve the steric interactions of the $Fe(CO)_4$ groups.

Synthesis and Reactivity of $[I]^{2-}$, $[II]^{2-}$, $[III]^{2-}$, and $[IV]^{2-}$. The syntheses of $[I]^{2-}$, $[II]^{2-}$, $[III]^{2-}$, and $[IV]^{2-}$ are all accomplished by a the same general method, reduction of a chalcogen oxide by KOH/$Fe(CO)_5$ in methanol solution. The fundamental parameter that determines whether the open or closed complexes are isolated is reaction time. At prolonged reaction times, $[II]^{2-}$ and $[IV]^{2-}$ are produced from $[I]^{2-}$ and $[III]^{2-}$, respectively. All of

(24) Schumann, H.; Magerstädt, M.; Pickardt, J. *J. Organomet. Chem.* **1982**, *240*, 407.
(25) Gervasio, G. *J. Organomet. Chem.* **1992**, *441*, 271.
(26) Mathur, P.; Reddy, V. D. *J. Organomet. Chem.* **1991**, *401*, 339.
(27) Bachman, R. E.; Whitmire, K. H. *J. Organomet. Chem.*, in press.
(28) Liaw, W.-F.; Chiang, M.-H.; Liu, C.-J.; Harn, P.-J.; Liu, L.-K. *Inorg. Chem.* **1993**, *32*, 1536.
(29) Luo, S.; Whitmire, K. H. *Inorg. Chem.* **1989**, *28*, 1424.
(30) Churchill, M. R.; Fettinger, J. C.; Whitmire, K. H.; Lagrone, C. B. *J. Organomet. Chem.* **1986**, *303*, 99.
(31) Etzrodt, G.; Boese, R.; Schmid, G. *Chem. Ber.* **1979**, *112*, 2574.
(32) Whitmire, K. H.; Lagrone, C. B.; Churchill, M. R.; Fettinger, J. C.; Biondi, L. V. *Inorg. Chem.* **1984**, *23*, 4227.
(33) Whitmire, K. H.; Leigh, J. S.; Gross, M. E. *J. Chem. Soc., Chem. Commun.* **1987**, 926.
(34) Dahl, L. F.; Sutton, P. W. *Inorg. Chem.* **1963**, *2*, 1067.
(35) Campana, C. F.; Lo, F. Y.-K.; Dahl, L. F. *Inorg. Chem.* **1979**, *18*, 3060.
(36) Mathur, P.; Hossain, M. M. *Organometallics* **1993**, *12*, 2398.

the anions can be easily isolated as $[PPN]^+$ salts by simple precipitation reactions, which produce high yields of relatively pure materials. These are important considerations if these materials are to be considered as reagents for further cluster-building reactions. We have only begun to probe the reactivity of these clusters, but several initial results are worthy of comment.

The synthesis of $[II]^{2-}$ from Te^{2-} and $Fe(CO)_5$ was recently reported.[1a] The fact that $[I]^{2-}$ converts to $[II]^{2-}$ over the course of several hours at room temperature and at a considerably faster rate at only moderately elevated temperatures implies that $[II]^{2-}$ may not be the initial product formed in the above reaction. Rather, it seems likely that $[I]^{2-}$ is formed first but is rapidly converted to $[II]^{2-}$ under the reaction conditions. This work also reports that the complex $[Te\{Fe(CO)_4\}_4]^{2-}$ results when an excess of $Fe(CO)_5$ is used.[1a] This compound can be readily derived from the reaction of $[I]^{2-}$ with "$Fe(CO)_4$" fragments. The stability of the open framework of this compound may be linked to the localization of the nonbonding electron pair by donation to the fourth $Fe(CO)_4$ fragment.

When the potassium salt of $[I]^{2-}$ is protonated in methanol, the major and minor products are the well-established clusters $Fe_3(CO)_9Te_2$ and $Fe_2(CO)_6Te_2$, respectively. This result strongly suggests that the initial species produced in Hieber's preparation of these clusters is $[I]^{2-}$. This conclusion conflicts with a recent report by Shieh and co-workers which identifies the initially formed cluster as $[Fe_8(CO)_{22}Te_6]^{2-}$ ($[V]^{2-}$).[37] This large cluster

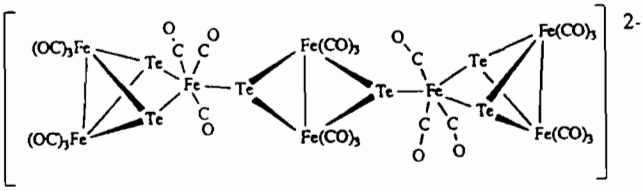

$[V]^{2-}$

consists of two $Fe_3(CO)_8Te_2$ fragments bridged by a $[Fe_2(CO)_6Te_2]^{2-}$ butterfly-shaped fragment. The results reported here show that this large cluster is not the initial product of the reaction of TeO_2 with $KOH/Fe(CO)_5/MeOH$. $[V]^{2-}$ is best understood in terms of the partial oxidation of $[I]^{2-}$ caused by the presence of adventitious oxygen. Partial oxidation would generate $Fe_3(CO)_9Te_2$ along with other fragments, such as $[Fe_2(CO)_6Te_2]^{2-}$, which may assemble to generate the observed product.

While the transformation of $[I]^{2-}$ to $[II]^{2-}$ is relatively slow at room temperature, the corresponding proceess is rapid for $[III]^{2-}$. The rapid rate of reaction for $[III]^{2-}$ indicates that this process must be energetically favorable. It was therefore worth investigating if the process could be reversed, particularly in the case of $[IV]^{2-}$. As a preliminary study, an acetonitrile solution of $[PPN]_2[IV]$ was placed under 1000 psi of CO at room temperature. No change was detectable by infrared spectroscopy after 3 days. Detailed kinetic data for the transformations of $[I]^{2-}$ to $[II]^{2-}$ and of $[III]^{2-}$ to $[IV]^{2-}$, as well as for other related compounds, are presently being collected to determine the activation parameters for these processes.

One last area deserving of comment is the use of $TeCl_4$ in the synthesis of $[II]^{2-}$. The reaction of $[Et_4N]_2[Fe_2(CO)_8]$ with $TeCl_4$ (2:1) in acetonitrile produces $[Et_4N]_2[II]$ in low yield along with at least one unidentified byproduct. It can be isolated in pure form by selective crystallization. This reaction is sensitive to many factors, including the ratio of reactants, the identity of the solvent, and the nature of the iron carbonylate anion employed.[38] Decreasing the $[Fe_2(CO)_8]^{2-}$:$TeCl_4$ ratio to 1:1 results in the clean formation of $Fe_2(CO)_6Te_2$ in high yield.[27] When this reaction is performed in THF, the only product is the known $Fe_3(CO)_9Te_2$. When $[Fe(CO)_4]^{2-}$ is employed instead of the dinulcear iron anion, the only product is again $Fe_3(CO)_9Te_2$, while reaction of either $[Fe_3(CO)_{11}]^{2-}$ or $[Fe_4(CO)_{13}]^{2-}$ with $TeCl_4$ has to date yielded only an intractable mixture of unidentified products.[38]

Conclusions

The use of methanolic KOH solutions of pentacarbonyliron has been shown to be fairly general for the synthesis of a wide variety of main group–iron clusters. Clusters containing elements from groups 13–15 prepared in this fashion have been widely studied. In almost all cases the initial reaction produces complexes of the general formula $[E\{Fe(CO)_4\}_x]^{n-}$ with $x = 2–4$ and $n = 0–3$. This has proven true for selenium and tellurium as well. These reactions allow for the preparation of reactive anionic clusters in high yield from inexpensive reagents. These considerations make these clusters ideal for use as reagents in the synthesis higher nuclearity homo- and heteronuclear clusters. The tendency of these open-framework clusters to convert to *closo* structures appears to be greatest when a nonbonding electron pair is present on the main group atom.

Acknowledgment. K.H.W. wishes to thank the National Science Foundation for financial support of this work and for assistance in the purchase of the diffractometer. R.E.B. thanks the NSF for a Predoctoral Fellowship. VG Analytical is acknowledged for providing the FABMS analyses.

Supplementary Material Available: Full tables of crystallographic details, bond metricals, and positional and anisotropic displacement parameters for $[PPN]_2[I]$, $[Et_4N]_2[II]$, and $[PPN]_2[IV]$ and diagrams of the other independent anions for $[PPN]_2[I]$ and $[Et_4N]_2[II]$ (62 pages). Ordering information is given on any current masthead page.

(37) Shieh, M.; Chen, P.-F.; Peng, S.-M.; Lee, G.-H. *Inorg. Chem.* **1993**, *32*, 3389.

(38) Bachman, R. E; Whitmire, K. H. Unpublished results.

(39) Delbaere, L. T. J.; Kruczynski, L. J.; McBride, D. W. *J. Chem. Soc., Dalton Trans.* **1973**, 307.

(40) Whitmire, K. H.; Leigh, J. S.; Luo, S.; Shieh, M.; Fabiano, M. D. *New J. Chem.* **1988**, *12*, 397.